Jordan Journal of Civil Engineering, Volume **5**, No. **2**, **2011**

Viscoplastic Finite Element Analysis of Complex Geotechnical Problems

Waddah Salman Abdullah

Associate Professor of Civil Engineering, Department of Civil Engineering, Jordan University of Science and Technology, Irbid, P.O. Box 3030, Jordan. E-Mail: waddah@just.edu.jo

ABSTRACT

The principles of elasto/viscoplastic finite element analysis were presented and explained, and the results and the analysis of some geotechnical problems were presented in this work. Plasticity models such as von-Mises, Tresca, Drucker-Prager and Mohr-Coulomb models with associated and non-associated flow rules were incorporated in the viscoplastic algorithm. The ultimate bearing capacity of a rigid surface footing on weightless clayey soil, Tresca material, predicted by the elasto/viscoplasticity approach agrees very well with that obtained by Prandtl exact solution (only 1% above Prandtl exact solution). Solution was also presented for complex problems with no available solution such as the problem of an anchor buried in sands (Mohr-Coulomb materials), where large zones within the soil domain are dominated by tensile stresses as well as sharp changes in shear stresses.

KEYWORDS: Viscoplasticity algorithm, Plasticity models, Associated flow rule, Non-associated flow rule, Foundations, Anchors.

INTRODUCTION

Soils are highly non-linear materials with anisotropic and inhomogeneous nature. Therefore, exact solutions for problems with such complex nature are not achievable. Early developments were to incorporate the non-linear elastic models such as the hyperbolic model in the finite element method (Kondner, 1963; Duncan and Chang, 1970). Other types of nonlinear functions such as the spline function were also incorporated in finite element analysis (Desai, 1971). Non-linear elasticity provided solutions, but with limited success. Nonlinear elasticity could not model or simulate soil dilation on shearing which is an important phenomenon for cohesionless soils. Accordingly, analysis incorporating such models experience immense deficiency in simulating and predicting soil deformations as well as stresses developed within soil domain due to applied loads and stresses. Plasticity modeling, however, represented an enormous step in pursuit of accurate prediction of soil behavior even under very complex stress systems such as tensile stresses and zones of very sharp changes in shear stresses. Early works on plasticity modeling with finite element method was mainly applied to metal stress analysis (Zienkiewicz and Nayak, 1971; Nayak and Zienkiewicz, 1972). Implementation of viscoplasticity with finite elements (Zienkiewicz and Cormeau, 1972, 1974; Cormeau, 1974) was intended for solving general problems in solid mechanics. Applications of viscoplasticity with finite elements using diversity of plasticity models were advanced, specifically for solving complex problems in geotechnical engineering (Abdullah, 1983, 1987a, 1987b, 2008). The various plasticity models used were; von-Mises, Tresca,

Accepted for Publication on 15/4/2011.

Drucker-Prager, Mohr-Coulomb, Rowe's stress-dilatancy model, and the critical state model, with associated and non-associated flow rules.

Scope of the Work

1. To illustrate the principles and implementation of the viscoplastic algorithm coupled with plasticity models in the finite element method.
2. To demonstrate the powerful nature of the elasto/viscoplastic approach for precise analysis of complex geotechnical engineering problems.

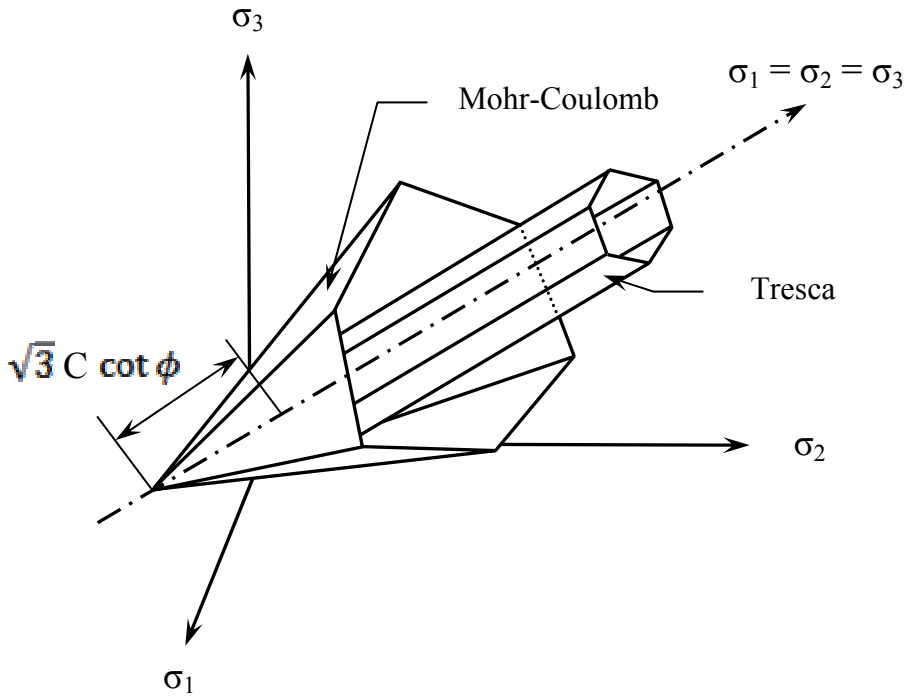

Figure 1: Mohr-Coulomb and Tresca plastic yield surfaces

PLASTICITY MODELS

The use of plasticity is intended to model the inelastic behavior of soils. This includes the detection of inelastic behavior, finding out the amount of irrecoverable strains and accounting for changes in material strength after plastic yielding had occurred; usually called hardening/softening (Nayak and Zienkiewicz, 1972; Zienkiewicz and Nayak, 1971; Zienkiewicz and Cormeau, 1972; Zienkiewicz and Cormeau, 1974; Cormeau, 1974; Abdullah, 1983, 1987a, 1987b, 2008). In a uniaxial stress system, the stress that limits elastic behavior is called the yield strength. In three- dimensional stress systems, plastic yielding is represented by a surface called the plastic yield surface, which separates the elastic state from the plastic state. There are several types of plastic yield surfaces. The shape of each of these surfaces is dependent on the type of soil it represents. Broadly speaking, the shapes of the plastic yield surfaces are divided into two categories. The first category is the hydrostatic stress independent surfaces, such as the von-Mises and Tresca surfaces which are appropriate for modeling cohesive soils (Fig.1, Fig. 2 and Fig.3). The second category is the hydrostatic stress dependent surfaces, such as Mohr-Coulomb and Drucker-Prager surfaces which are appropriate for cohesionless soils or mixed soils (Fig.1, Fig. 2 and Fig.3). Mathematically,

the plastic yield surface (Table 1) is represented by,

$$F(\sigma, \varepsilon, \kappa) = 0 \quad (1)$$

where: σ represents the stress components, ε^p represents the accumulated plastic strains and κ is the hardening coefficient.

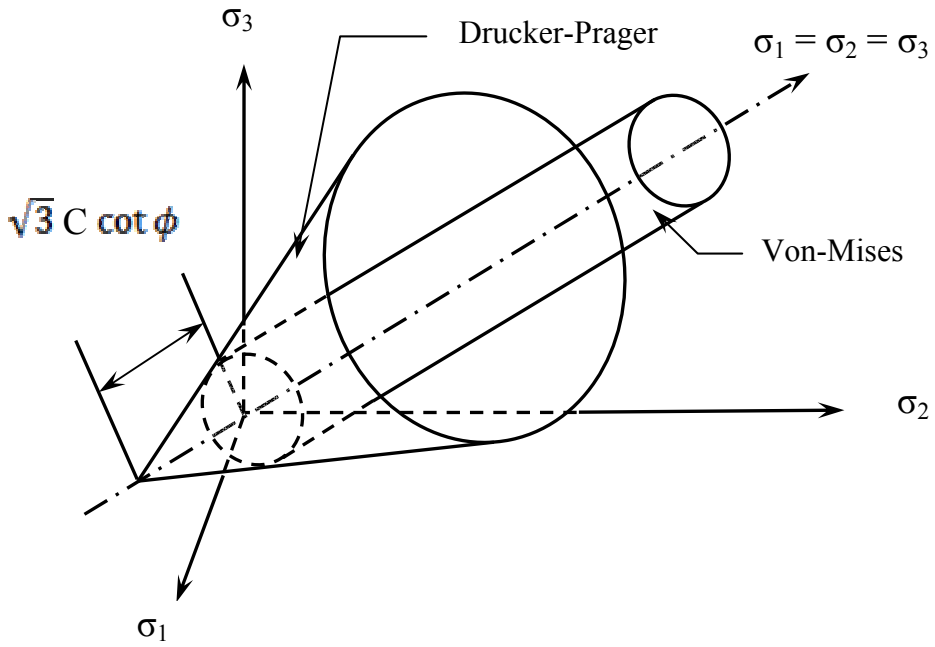

Figure 2: Drucker-Prager and Von-Mises plastic yield surfaces

Mohr-coulomb and Tresca plastic yield surfaces and Drucker-Prager and von-Mises plastic yield surfaces are shown in Fig.1 and Fig.2, respectively. The π-plane of some commonly used plastic yield functions is shown in Fig. 3.

The conditions for F are;

F < 0.0	Elastic state of stress;
F = 0.0	Plastic flow;
F > 0.0	Not permitted.

The flow theory of plasticity establishes a relationship between increments of stress and strain rates, usually known as "normality condition". The latter does not give the magnitude of plastic strain but establishes the ratio of the strain components, such that;

$$d\epsilon^p \propto \frac{\partial Q}{\partial [\sigma]} \quad (2)$$

and $$d\epsilon^p = d\lambda \frac{\partial Q}{\partial [\sigma]} \quad (3)$$

where: Q is the plastic potential function and may be represented in a fashion similar to the plastic yield surface (Eq. 1). $d\lambda$ is a non-negative proportionality constant which may vary throughout the loading history.

The plastic potential may assume the same function as that of the plastic yield function, and in this case we have what is commonly known as "associated flow rule", such that;

$$Q \equiv F \quad (4)$$

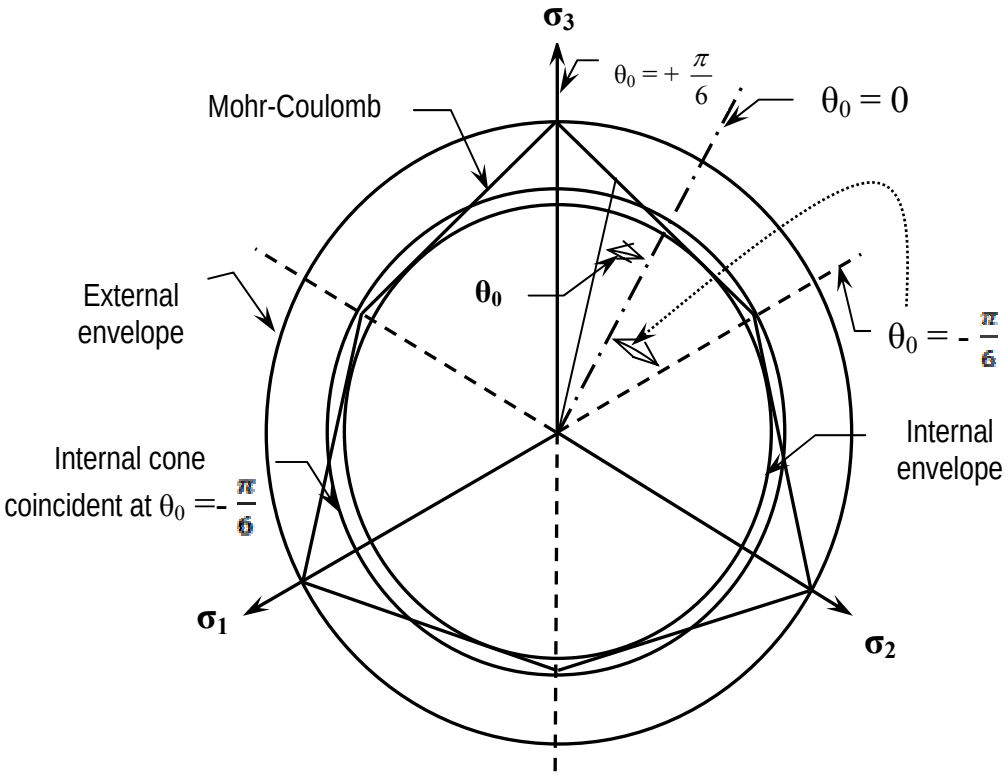

Figure 3: π-plane for some commonly used plastic yield functions

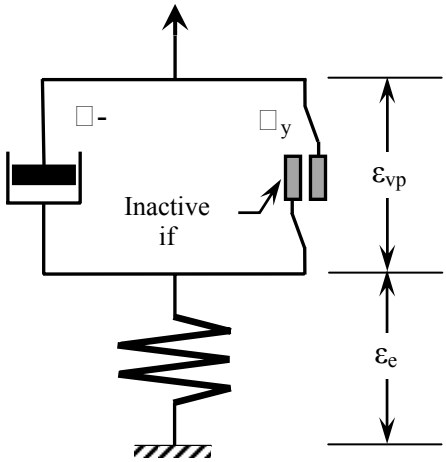

Figure 4: One-dimensional elasto/viscoplastic model

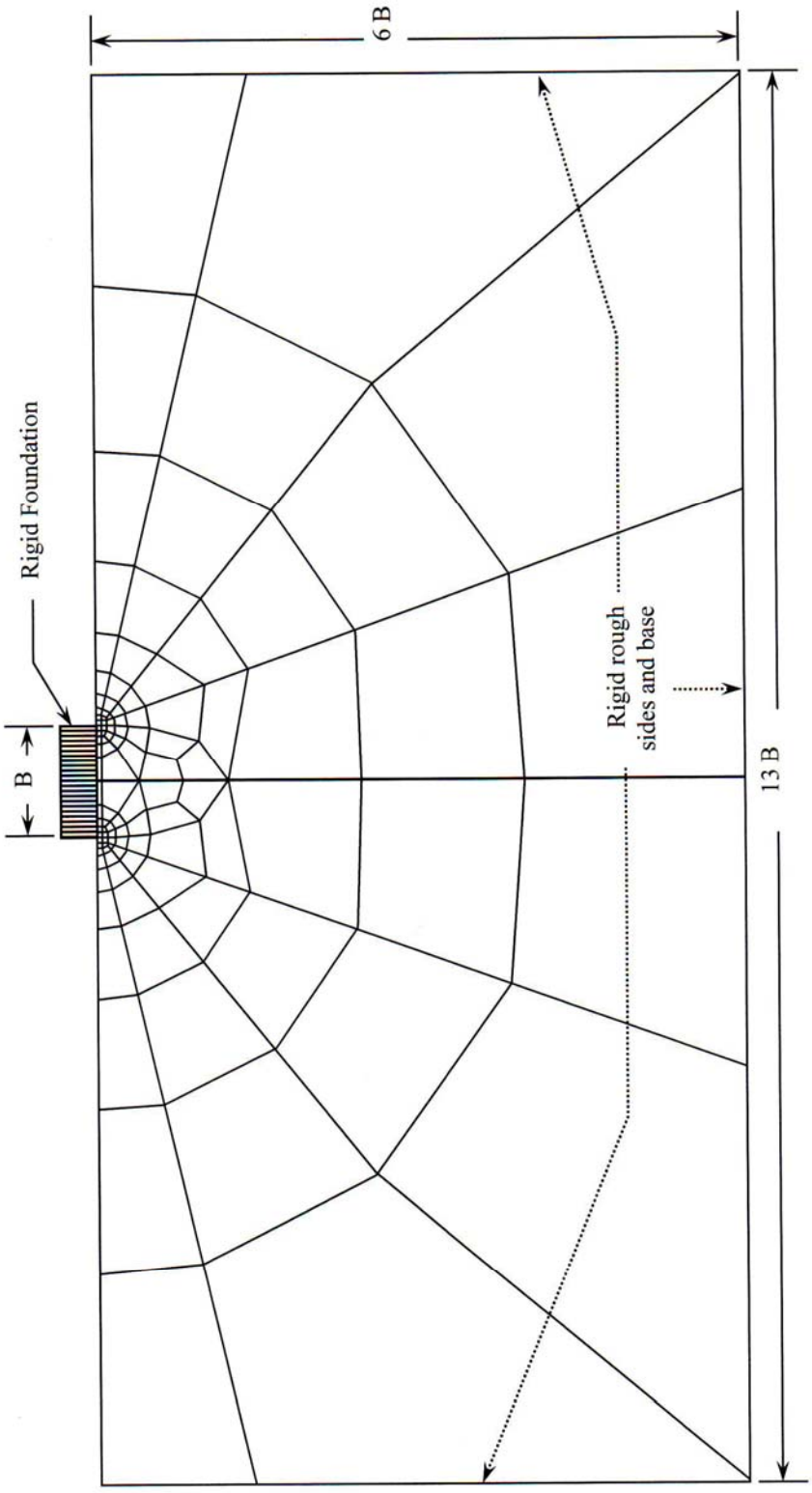

Figure 5: The finite element mesh used to demonstrate the efficiency of the viscoplastic approach (Abdullah, 1983)

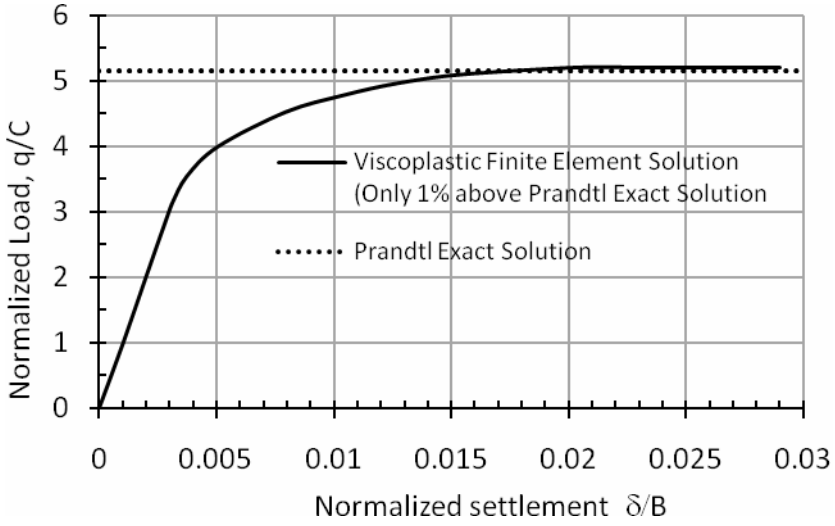

Figure 6: Load settlement relationship for a rigid smooth foundation on weightless soil; Tresca yield criterion, Plane strain condition, critical time stepping (Abdullah, 1983)

Changes in the state of the yield surface whether in shape, size and location compared to its previous state are loosely called "hardening". Hardening is called isotropic if and only if the size of the plastic yield surface changes, whilst the location and shape does not change. On the other hand, hardening is called "kinematic" if the location of the yield surface translates along the direction of the plastic strain increment.

Isotropic hardening usually involves one simple parameter denoting the state of the material. If plastic work is used as the hardening parameter, the process is called "Work-Hardening". It establishes a relationship between the plastic work done by the external agency and the hardening produced by the plastic deformation, which is eventually related to the parameter κ (Eq. 1), such that;

$$W_p = \int [\sigma]\, d[\varepsilon^p] \tag{5}$$

where: W_p is the amount of plastic work per unit volume. However, the rate of plastic work may be positive, zero or even negative depending on the type and state of the material. Negative rate of plastic work signifies softening rather than hardening.

If the accumulated plastic strain is taken as the measure of hardening, then the process is known as "Strain Hardening". It establishes a relationship between the accumulated plastic strain and hardening, which is related to parameter κ (Eq. 1), such that;

$$H = F\left(\int d\,[\varepsilon^p]\right) \tag{6}$$

H is always an increasing function of plastic strain. However, the rate of H may become negative as in the case of softening. The incremental plastic stress-strain law may be given directly from the normality principle (Eq. 3), such that;

$$d\varepsilon^p = d\lambda \frac{dQ}{d[\sigma]} = d\lambda\, \bar{a} \tag{7}$$

and

$$\bar{a} = \begin{bmatrix} \frac{\partial Q}{\partial \sigma_x} \\ \frac{\partial Q}{\partial \sigma_y} \\ \vdots \end{bmatrix} \quad \text{or} \quad \bar{a} = \frac{\partial Q}{\partial \sigma_m}\frac{\partial \sigma_m}{\partial [\sigma]} + \frac{\partial Q}{\partial \bar{\sigma}}\frac{\partial \bar{\sigma}}{\partial [\sigma]} + \frac{\partial Q}{\partial \sigma_\theta}\frac{\partial \sigma_\theta}{\partial [\sigma]} \tag{8}$$

and

$$\frac{\partial \theta_\sigma}{\partial [\sigma]} = -\frac{\sqrt{3}}{2\cos 2\theta_\sigma}\left[\frac{1}{\bar{\sigma}^3}\frac{\partial J_3}{\partial [\sigma]} - \frac{3J_3}{\bar{\sigma}^4}\frac{\partial \bar{\sigma}}{\partial [\sigma]}\right] \tag{9}$$

Equation 8 may be rewritten as;

$$\bar{a} = [B][\bar{a}]^T \text{ or } \bar{a} = B_1\bar{a}_1 + B_2\bar{a}_2 + B_3\bar{a}_3 \quad (10)$$

where, $\bar{a}_1, \bar{a}_2$ *and* $\bar{a}_3$ are the derivatives of $\sigma_m, \bar{\sigma}$ *and* J_3 with respect to the components of stresses and such that;

$$\frac{\partial \sigma_m}{\partial [\sigma]} = \bar{a}_1 = \frac{1}{3}\begin{bmatrix}1\\1\\1\\0\\0\\0\end{bmatrix}; \quad \frac{\partial \bar{\sigma}}{\partial [\sigma]} = \bar{a}_2 = \frac{1}{2\bar{\sigma}}\begin{bmatrix}S_x\\S_y\\S_z\\2\tau_{yz}\\2\tau_{xz}\\2\tau_{xy}\end{bmatrix};$$

$$\frac{\partial J_3}{\partial [\sigma]} = \bar{a}_3 = \begin{bmatrix}S_yS_z - \tau_{yz}^2\\S_{xy}S_z - \tau_{xz}^2\\S_xS_y - \tau_{xy}^2\\2(\tau_{xz}\tau_{xy} - S_x\tau_{yz})\\2(\tau_{xy}\tau_{yz} - S_y\tau_{xz})\\2(\tau_{yz}\tau_{xy} - S_z\tau_{xy})\end{bmatrix} + \frac{1}{3}\bar{\sigma}\begin{bmatrix}1\\1\\1\\0\\0\\0\end{bmatrix} \quad (11)$$

θ_0, σ_m, $\bar{\sigma}$, S_x, S_y, S_z and J_3 are given in the Appendix.

B_1, B_2 and B_3 are constant parameters related to a particular plastic yield function (Table 2).

Viscoplasticity Algorithm

Viscoplasticity is a physically more logical approach for simulating material inelasticity behavior than the plasticity approach. Moreover, numerically the viscoplastic approach eliminates some numerical difficulties associated with the elasto-plastic modeling, such as strain softening and non-associated flow rules. The time factor involved in the viscoplastic model may be used to obtain real time dependent solutions, given that the parameters involved in the model are experimentally determined. It could also be used as a pure computational artifice leading to an elasto/plastic solution (Nayak and Zienkiewicz, 1972; Zienkiewicz and Nayak, 1971; Zienkiewicz and Cormeau, 1972; Zienkiewicz and Cormeau, 1974; Cormeau, 1974; Abdullah, 1983, 1987a, 1987b, 2008).

The concept of the elasto/viscoplastic modeling is that the material behaves elastically on loading as long as the stresses stay within the plastic yield function (F<0). Beyond that, there is an additional time dependent component of strains (called viscoplastic) the rate of which is dependent on the amount of excess stress beyond the plastic yield surface. Therefore, the total strain rate may be obtained as;

$$[\dot{\varepsilon}] = [D]^{-1}[\dot{\sigma}] + \gamma \langle \phi(F)^{\delta} \rangle \frac{\partial Q}{\partial [\sigma]} \quad (12)$$

where: [*D*] = elasticity matrix, γ= fluidity parameter, *F* = plastic yield function and *Q* = plastic potential function.

Also, the following means;

$$\langle \phi(F)^{\delta} \rangle = 0 \quad \text{for } F < 0 \quad (13a)$$

$$\langle \phi(F)^{\delta} \rangle = \phi(F)^{\delta} \quad \text{for } F > 0 \quad (13b)$$

For a uniaxial model, the viscoplastic concept is shown in Fig. 4. It consists of an elastic spring connected in parallel with a Bingham unit, which consists of a plastic unit capable of taking a stress σ_y and a dashpot. The total stress σ may exceed the yield value σ_y by an amount, which is a fact that has a physical justification (Perzyna, 1966) and is the fundamental difference between plasticity and viscoplasticity. The plastic yield surface *F*, the plastic potential surface *Q*, the normality condition and the hardening/softening phenomenon have the same meaning as in the context of plasticity. The function *F* may assume a number of forms, linear, exponential, logarithmic …etc. The linear form of $(\phi(F)^{\delta} = F)$ is fairly adequate to describe the behavior of many materials (Zienkiewicz and Cormeau, 1972; Abdullah, 1983). The viscoplastic solution involves the integration of matrix equations in time. There are a large number of these stepping schemes. Euler's forward time marching scheme has been shown to be efficient (Cormeau, 1974; Abdullah, 1983). In this scheme, it is assumed that

viscoplastic strain rate $\dot{\varepsilon}^{vp}$ remains constant within each time interval after it has been determined from a state of stress assumed to remain constant at the beginning of that time interval. Numerical instability may occur if the time interval length is too large. Firstly empirical rules were introduced (Zienkiewicz, and Cormeau, 1972, 1974), such as;

$$\Delta t \leq \tau \frac{\|\varepsilon\|}{\|\dot{\varepsilon}^{vp}\|} \tag{14}$$

and

$$\Delta t \leq \tau \frac{\|\bar{\varepsilon}\|}{\|\dot{\bar{\varepsilon}}^{vp}\|} \tag{15}$$

where;

$$\|\varepsilon\| = \sqrt{\varepsilon_1^2 + \varepsilon_2^2 + \varepsilon_3^2} \tag{16a}$$

$$\|\dot{\varepsilon}^{vp}\| = \sqrt{(\dot{\varepsilon}_1^{vp})^2 + (\dot{\varepsilon}_2^{vp})^2 + (\dot{\varepsilon}_3^{vp})^2} \tag{16b}$$

$$\|\bar{\varepsilon}^{vp}\| = \sqrt{\left[\frac{2}{3}\left\{(\varepsilon_x^{vp})^2 + (\varepsilon_y^{vp})^2 + (\varepsilon_z^{vp})^2\right\} + \frac{1}{3}\left\{(\gamma_x^{vp})^2 + (\gamma_y^{vp})^2 + (\gamma_z^{vp})^2\right\}\right]} \tag{16c}$$

$$\|\dot{\bar{\varepsilon}}^{vp}\| = \sqrt{\left[\frac{2}{3}\left\{(\dot{\varepsilon}_x^{vp})^2 + (\dot{\varepsilon}_y^{vp})^2 + (\dot{\varepsilon}_z^{vp})^2\right\} + \frac{1}{3}\left\{(\dot{\gamma}_x^{vp})^2 + (\dot{\gamma}_y^{vp})^2 + (\dot{\gamma}_z^{vp})^2\right\}\right]} \tag{16d}$$

It was found from numerical experiments that τ values ranging from 0.01 to 0.15 gave stable solutions. Experiments have shown that none of the empirical rules was satisfactory as far as stability and economy of the solution were concerned. For associated flow rules, and based on the viscous properties of the material, a critical time interval length was obtained (Zienkiewicz and Cormeau, 1974). For von-Mises, Tresca and Mohr-Coulomb plastic yield functions, the critical time interval length is given as;

Von-Mises $$\Delta t_{crit} \leq \frac{4(1+\nu)}{3\gamma E} \tag{17a}$$

Tresca $$\Delta t_{crit} \leq \frac{1+\nu}{\gamma E} \tag{17b}$$

Mohr-Coulomb

$$\Delta t_{crit} \leq \frac{(1+\nu)(1-2\nu)}{\gamma E[1-2\nu+(\sin\phi)^2]} \tag{17c}$$

where: E = modulus of elasticity, ν = Poisson's ratio, ϕ = friction angle and γ = fluidity parameter.

VERIFICATION OF THE VISCOPLASTIC APPROACH

In order to demonstrate the powerful nature of the viscoplastic approach, a rigid strip surface footing resting on weightless clayey soil was considered. Prandtl (1920 and 1921) obtained an exact analytic solution for a rigid strip surface footing resting on

weightless clayey soil. Prandtl (1920 and 1921) found that yielding occurs at a bearing pressure equal to πC, and the ultimate bearing capacity $q_u = (2+\pi)$ C or $q_u/C = (2+\pi)$; (C is the soil cohesion).

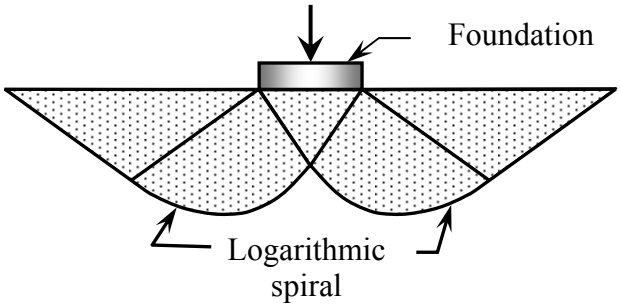

Figure 7: Failure mechanism for surface footing elasto-viscoplastic approach and Prandtl solution (Abdullah, 1983)

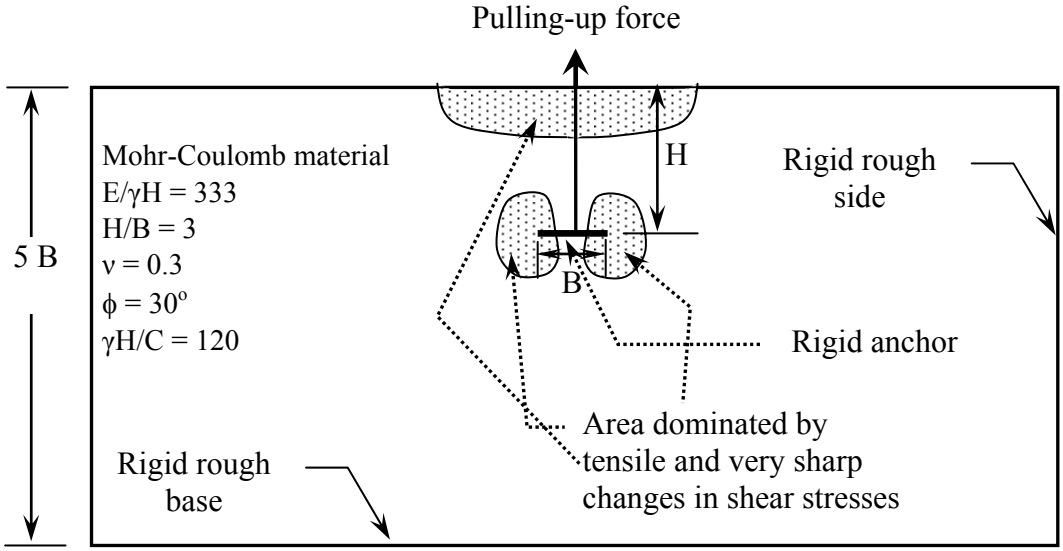

Figure 8: Vertically pulled rigid anchor

For the elasto/viscoplastic finite element solution, the soil domain was idealized with a carefully designed finite element mesh (Fig. 5). The mesh provided small-sized elements at areas of load discontinuity and very sharp shear stress changes in order to account for such sharp changes. The finite elements used were 8-noded isoparametric elements, and the material was modeled as Tresca type material (Abdullah, 1983). The ultimate bearing capacity predicted by the viscoplastic finite element approach (Abdullah, 1983) yielded an excellent result (Fig. 6) as compared with Prandtl exact solution (only 1% above Prandtl exact solution). The load settlement relationship (Fig. 6) for the rigid strip surface footing resting on weightless clayey soil demonstrates that initial yielding started at $q/C = \pi$ as predicted by Prandtl exact solution (Abdullah, 1983). The plastic zone or the failure mechanism predicted by Prandtl exact method and the plastic zone predicted by the viscoplastic finite element solution (Fig. 7) are both identical (Abdullah, 1983).

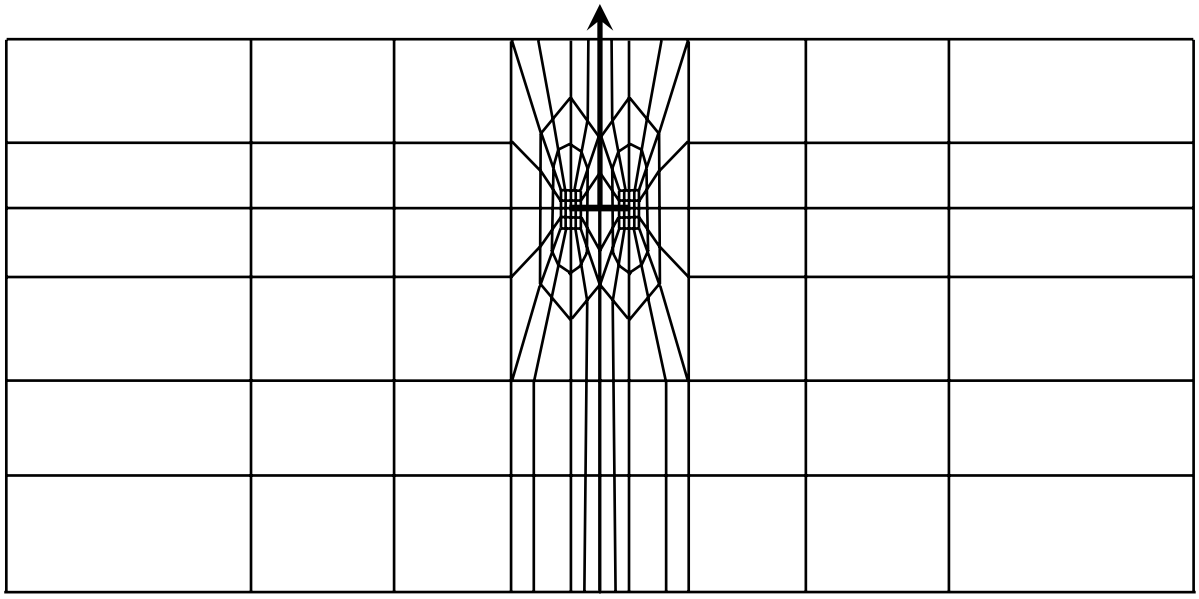

Figure 9: Finite element mesh for the anchor problem (Abdullah, 1983)

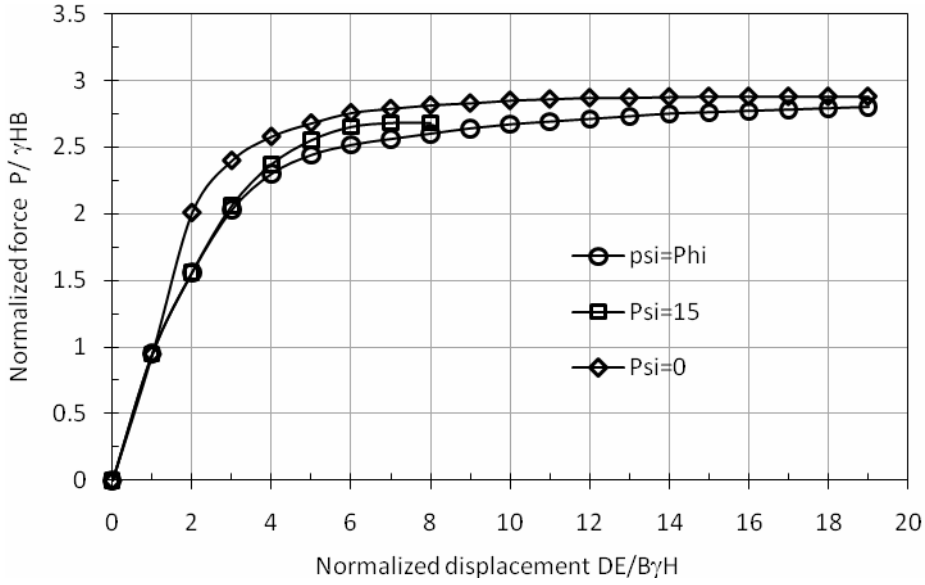

Figure 10: Load displacement relationships for the anchor problem (Abdullah, 1983)

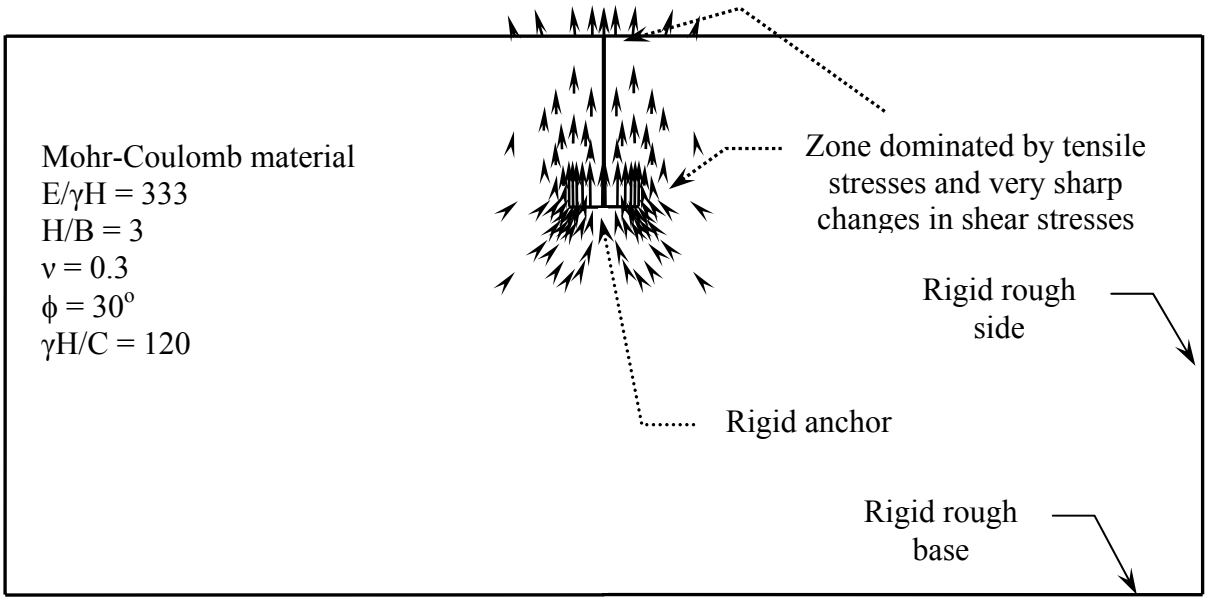

Figure 11: Vector displacement field for the anchor problem (Abdullah, 1983)

Table 1: Common plasticity models

Type of plastic model	Plastic yield function
Von-Mises	$F = \sqrt{3}\,\bar{\sigma} - Y = 0$
Tresca	$F = 2\bar{\sigma}\,\cos\theta_0 - Y = 0$
Drucker-Prager	$F = 3\,\acute{\alpha}\,\sigma_m + \bar{\sigma} - k = 0$ $\acute{\alpha} = \frac{2\sin\phi}{\sqrt{3}\,(3-\sin\phi)};\; k = \frac{6\,C\cos\phi}{\sqrt{3}\,(3-\sin\phi)}$
Mohr-Coulomb	$F = \sigma_m \sin\phi + \bar{\sigma}\,\cos\theta_0 - \frac{\bar{\sigma}}{\sqrt{3}}\sin\theta_0\,\sin\phi - C\,\cos\phi$

Table 2: Parameters for some common plasticity models

Plastic model	B_1	B_2	B_3
Von-Mises	0	$\sqrt{3}$	0
Tresca	0	$2\cos\theta_0(1+\tan\theta_0\tan 3\theta_0)$	$\frac{\sqrt{3}}{\bar{\sigma}^2}\frac{\sin\theta_0}{\cos 3\theta_0}$
Drucker-Prager	$3\acute{\alpha}$	1.0	0
Mohr-Coulomb	$\sin\phi$	$\cos\theta_0\left[(1+\tan\theta_0\tan 3\theta_0)+\frac{\sin\phi}{\sqrt{3}}(\tan 3\theta_0-\tan\theta_0)\right]$	$\frac{\sqrt{3}\left[\sin\theta_0+\left(\frac{1}{\sqrt{3}}\right)\cos\theta_0\sin\phi\right]}{2\bar{\sigma}^2\cos 3\theta_0}$

Undoubtedly, this example demonstrated that the elasto/viscoplastic finite element solution yielded very accurate results as far as initial yielding, ultimate bearing capacity and failure mechanism were concerned. Therefore, for any type of geotechnical problem where no exact solution is available, the elasto/viscoplastic finite element approach may be used to obtain a high precision solution.

ANCHOR PROBLEM

The second problem considered in this work was the anchor problem where, due to its complex nature, there is no available exact solution. In addition to the plastic nature of soils, the anchor problem produces large areas dominated by tensile stresses and very sharp changes in shear stresses (Fig. 8) which render the problem as insolvable by any analytical method. The soil domain was idealized by an appropriate finite element mesh (Fig. 9), that takes into account the very sharp changes in shear stresses as designated by the problem description (Fig. 8). The finite elements used were 8-noded is oparametric elements and the material was modeled by Mohr-Coulomb yield criterion (Abdullah, 1983). The normalized force *versus* normalized vertical displacement for an associated flow rule and a non-associated flow rule ($\psi = 15°$, and $\psi = 0°$) differs, fairly, in behavior up till near failure, getting closer at later stages of loading, where the effect of dilation due to associated flow rule diminishes more and more at later stages(Fig. 10). The displacement field for the anchor problem shows a large amount of movements around the anchor as well as at the soil surface right above the anchor (Fig. 11).

SUMMARY AND CONCLUSIONS

Soils are highly nonlinear materials, therefore, assuming soils as linear elastic materials produces a gross amount of error. Non-linear elasticity was introduced, but only with limited success. Plasticity models incorporated in finite element analysis yielded solutions with a great deal of accuracy. Viscoplasticity approach is more realistic than plasticity in terms of reproducing actual material behavior and yields highly accurate results even for very complex problems. In this work, the viscoplasticity modeling and algorithm were incorporated in the finite element method (8-noded isoparametric elements). Various plasticity models were incorporated. These were; von-Mises, Tresca, Drucker-Prager, Mohr-Coulomb, Rowe's stress-dilatancy model and the critical state model, with associated and non-associated flow rules. Evaluation of the performance of the viscoplasticity analysis was conducted on a problem with known exact solution. The considered problem was a rigid surface footing resting on a cohesive weightless soil (Tresca type material, $\phi = 0$). Prandtl provided exact solution for the mentioned problem with the ultimate bearing capacity $q_u = (2+\pi)$ C. The elasto/viscoplastic finite element solution was in very close agreement with Prandtl exact solution (only 1% above the exact solution). This kind of result represents significant development for finding highly accurate results for very complex geotechnical problems which have no known exact solutions. The anchor problem represents one such complex problem with zones dominated by tensile stresses as well as very sharp changes in shear stresses.

APPENDIX

θ_0 = Lode angle, and is given as;

$$\theta_0 = \frac{1}{3}\sin^{-1}\left[-\frac{3\sqrt{3}}{2}\frac{J_3}{\bar{\sigma}^3}\right] \quad \text{with}$$

$$-\frac{1}{6}\pi \leq \theta_0 \leq \frac{1}{6}\pi \qquad \text{(A1)}$$

$$\sigma_m = \frac{1}{3}(\sigma_x + \sigma_y + \sigma_z) \qquad \text{(A2)}$$

$$\bar{\sigma} = \sqrt{\frac{1}{2}\left(S_x^2 + S_y^2 + S_z^2\right) + \tau_{xy}^2 + \tau_{yz}^2 + \tau_{zx}^2} \qquad \text{(A3)}$$

$S_x = \sigma_x - \sigma_m \quad S_y = \sigma_y - \sigma_m \quad S_z = \sigma_z - \sigma_m$ and $J_3 = S_x S_y S_z + 2\tau_{xy} \tau_{yz} \tau_{zx} - S_x \tau_{yz}^2 - S_y \tau_{xz}^2 - S_z \tau_{xy}^2$ (A4)

REFERENCES

Abdullah, W.S. 2008. New elastoplastic method for calculating the contact pressure distribution under rigid foundations, *Jordan Journal of Civil Engineering*, 2 (1), January.

Abdullah, W.S. 1987a. Shakedown analysis of footings on elastoplastic continua, Proceedings of the Second Arab Conference on Structural Engineering, Jordan University, Department of Civil Engineering, pp.32/1-32/25, 19-22 April, Amman.

Abdullah, W.S. 1987b. Vertically pulled anchors buries in no-tension materials, Proceedings of the Second Arab Conference on Structural Engineering, Jordan University, Department of Civil Engineering, pp.29/1-29/17, 19-22 April, Amman.

Abdullah, W.S. 1983. Non-linear finite element analysis of shallow footings, Ph.D. thesis submitted to the University of Wales, School of Engineering, Division of Civil Engineering, University College of Swansea, Wales.

Cormeau, I.C. 1974. Viscoplasticity and plasticity in the finite element method, Ph.D. Thesis, University College of Swansea, Wales.

Desai, C.S. 1971. Nonlinear analysis using spline functions, *Journal of the Soil Mechanics and Foundations Division, ASCE*, 97 (SM10): 1461-1480.

Duncan, J.M. and Chang, C.Y. 1970. Nonlinear analysis of stress and strain in soils, *Journal of the Soil Mechanics and Foundations Division, ASCE,* 96 (SM5).

Kondener, R.L. 1963. Hyperbolic stress-strain response: cohesive soils, *Journal of the Soil Mechanics and Foundations Division, ASCE*, 89 (SM10): 115-143.

Nayak, G.C. and Zienkiewicz, O.C. 1972. Elasto-plastic stress analysis. A generalization for various constitutive relations including strain softening, *International Journal for Numerical Methods in Engineering*.

Perzyna, P. 1966. Fundamental problems in visco-plasticity. Recent advances in applied mechanics, Academic Press, 9, New York.

Prandtl, L. 1920. Über die Härte plastischer Körper, *Nachr. K. Ges. Wiss.* Gött., Math.-Phys., Kl, 74-85.

Prandtl, L. 1921. Über die Eindringungsfestigkeit (Härte) plastischer Baustoffe und die Festigkeit von Schneiden, *Z. Angew. Math. Mech.,* 15-20.

Zienkiewicz, O.C. and Nayak, G.C. 1971. A general approach to problems of large deformation and plasticity using isoparametric elements, 3rd Conference on Matrix Methods, Wright-Patterson Air Force Base, Ohio.

Zienkiewicz, O.C. and Cormeau, I.C. 1972. Viscoplasticity solution by finite element process, *Archives of Mechanics*, 24 (5-6): 873-889, Warszawa.

Zienkiewicz, O.C. and Cormeau, I.C. 1974. Viscoplasticity-plasticity and creep in elstic solids – a unified numerical solution approach, *International Journal for Numerical Methods in Engineering*, 8: 821-845.